Investigation of the suitability of silicate bonding for facet termination in active fiber devices

Supriyo Sinha,[1] Karel E. Urbanek,[1] Alan Krzywicki,[2] and Robert L. Byer[1]

[1]*Edward L. Ginzton Laboratory, Stanford University, 450 Via Palou, Stanford, CA 94305, USA*

[2]*Rochester Institute of Technology, One Lomb Memorial Drive, Rochester, NY 14623, USA*

supriyo@stanford.edu

Abstract: We demonstrate that silicate bonding an optical flat to the output facet of an active fiber device can increase the reliability of high-peak power systems and subsantially reduce the effective feedback at the termination of a double-clad fiber. We determine the bonding parameters and conditions that maximize the optical damage threshold of the bond and minimize the Fresnel reflection from the bond. At 1-μm wavelength, damage thresholds greater than 70 J/cm^2 are demonstrated for 25-ns pulses. We also measured Fresnel reflections less than -63 dB off the bond. Finally, we determined that the strength of the bond is sufficient for most operating environments.

OCIS codes: (060.2320) Fiber optics amplifiers and oscillators; (140.3330) Laser damage; (240.0240) Optics at surfaces; (350.1820) Damage.

References and links

1. V. Gapontsev, D. Gapontsev, N. Platonov, O. Shkurikhin, V. Fomin, A. Mashkin, M. Abramov, and S. Ferin, "2 kW CW ytterbium fiber laser with record diffraction-limited brightness," Conference on Lasers and Electro-Optics Europe, CLEO/Europe (2005).
2. C. Brooks and F. Di Teodoro, "Multimegawatt peak-power, single-transverse-mode operation of a 100 μm core diameter, Yb-doped rodlike photonic crystal fiber amplifier," Appl. Phys. Lett. **89**, 111,119 (2006).
3. N. Bloembergen, "Role of cracks, pores, and absorbing inclusions on laser induced damage threshold at surface of transparent dielectrics," Appl. Opt. **12**, 661 (1973).
4. M. Wickham, J. Anderegg, S. Brosnan *et al.*, "Coherently coupled high power fiber arrays," Advanced Solid State Photonics, Santa Fe, USA, February pp. 1–4 (2004).
5. J. Nilsson, J. Sahu, Y. Jeong, W. Clarkson, R. Selvas, A. Grudinin, and S. Alam, "High Power Fiber Lasers: New Developments," Proceedings of SPIE (Photonics West) **4974**, 50–60 (2003).
6. S. Sinha, C. Langrock, M. Digonnet, M. Fejer, and R. Byer, "Efficient yellow-light generation by frequency doubling a narrow-linewidth 1150 nm ytterbium fiber oscillator," Opt. Lett. **31**, 347–349 (2006).
7. S. Sinha, K. Urbanek, D. Hum, M. Digonnet, M. Fejer, and R. Byer, "Linearly polarized, 3.35 W narrow-linewidth, 1150 nm fiber master oscillator power amplifier for frequency doubling to the yellow," Opt. Lett. **32**, 1530–1532 (2007).
8. D. Gwo, "Ultra precision and reliable bonding method," (2001). US Patent 6,284,085.
9. E. Elliffe, J. Bogenstahl, A. Deshpande, J. Hough, C. Killow, S. Reid, D. Robertson, S. Rowan, H. Ward, and G. Cagnoli, "Hydroxide-catalysis bonding for stable optical systems for space," Class. Quantum Grav. **22**, S257–S267 (2005).
10. P. Sneddon, S. Bull, G. Cagnoli, D. Crooks, E. Elliffe, J. Faller, M. Fejer, J. Hough, and S. Rowan, "The intrinsic mechanical loss factor of hydroxy-catalysis bonds for use in the mirror suspensions of gravitational wave detectors," Class. Quantum Grav. **20**, 5025–5037 (2003).

#86286 - $15.00 USD Received 10 Aug 2007; revised 14 Sep 2007; accepted 24 Sep 2007; published 25 Sep 2007

11. K. Mackenzie, I. Brown, P. Ranchod, and R. Meinhold, "Silicate bonding of inorganic materials Part 1. Chemical reactions in sodium silicate at room temperature," J. Mater. Sci. **26**, 763–768 (1991).
12. J. Limpert, A. Liem, H. Zellmer, A. Tunnermann, S. Knoke, and H. Voelckel, "High-average-power millijoule fiber amplifier system," Lasers and Electro-Optics, 2002. CLEO'02. Technical Digest. pp. 591–592 (2002).
13. D. Marcuse, "Gaussian approximation of the fundamental modes of graded-index fibers," J. Opt. Soc. Am. **68**, 103–109 (1978).
14. A. E. Siegman, "Lasers," Lasers, (University Science Books, 1986), Vol. 1283 pp, 1986.
15. J. Limpert, F. Roser, T. Schreiber, and A. Tunnermann, "High-power ultrafast fiber laser systems," IEEE J. Sel. Top. Quantum Electron. **12**, 233–244 (2006).
16. B. Stuart, M. Feit, S. Herman, A. Rubenchik, B. Shore, and M. Perry, "Nanosecond-to-femtosecond laser-induced breakdown in dielectrics," Phys. Rev. B **53**, 1749–1761 (1996).
17. S. Nemoto and T. Makimoto, "Analysis of splice loss in single-mode fibres using a Gaussian field approximation," Opt. Quantum Electron. **11**, 447–457 (1979).
18. S. Hansen, K. Dybdal, and C. Larsen, "Gain limit in erbium-doped fiber amplifiers due to internal Rayleigh backscattering," IEEE Photon. Technol. Lett. **4**, 559–561 (1992).
19. J. Smith, G. Harry, J. Betzwieser, A. Gretarsson, D. Guild, S. Kittelberger, M. Mortonson, S. Penn, and P. Saulson, "Mechanical loss associated with silicate bonding of fused silica," Class. Quantum Grav. **20**, 5039–5047 (2003).
20. H. Armandula and P. Willems, "Fused silica fibers - silicate bonding research at Caltech," Proceedings of ALUK meeting **ALUKGLA0017aAUG03**, 1–17 (2003).
21. B. Abott and R. Abott and R. Adhikari and A. Ageev and and B. Allen and R. Amin and S. Anderson and others, "Detector description and performance for the first coincidence observations between LIGO and GEO," Nucl, Inst. Meth. Phys. Research, A **517**, 154–179 (2004).

1. Introduction

In the last decade, the power levels demonstrated with high-power fiber laser sources have increased substantially. This has largely been enabled by the use of double-clad fiber geometries that allow the output power from high-power laser-diode stacks to be efficiently coupled into the fiber gain medium. The small mode area in fiber lasers compared to conventional solid-state bulk gain media allow for small saturation powers and low laser thresholds. CW powers greater than 2 kW in a diffraction-limited beam has been recently demonstrated from ytterbium-doped fiber lasers [1].

However, the high output intensities at the output facet for high-power fiber sources, due to the small mode field area of the fiber, can limit the power scalability of fiber lasers and amplifiers, and constitutes one of the disadvantages of fiber lasers compared to traditional bulk solid-state gain media. Although output peak powers as high as 4.5 MW in nanosecond pulses and output intensities of nearly 80 GW/cm^2 have been measured [2], these results have only been demonstrated in carefully controlled environments with no long-term reliability data. Commercial fiber sources offer considerably lower peak powers due to concerns of facet damage.

There are two reasons for the lower damage threshold of the silica-fiber facet compared to that of the bulk. First, it is well known that the presence of surface states and submicroscopic cracks and pores at the surface of a dielectric result in a reduced damage threshold at the surface compared to the bulk, by a factor of at least 2 [3]. These cracks and pores are present even for vacuum-cleaved fibers or chemically-polished facets. The presence of dopant ions in the core can also negatively impact the damage threshold, but this is a smaller effect. Second, contamination of the fiber end can further reduce the damage threshold, by up to several orders of magnitude. It is for this latter reason that researchers have found experimentally that the intensity at the output of the fiber should be limited to 65 MW/cm^2 for long-term CW operation at 1064 nm [4], even though the CW bulk-damage threshold for pure fused silica at this wavelength is two orders of magnitude higher [5]. We demonstrate in this paper how attaching an optical flat to a fiber end via silicate bonding can substantially improve the reliability of high-power fiber sources.

Since active fiber devices typically have high single-pass gains, it is important to tightly limit the optical feedback into such gain media to obtain the desired output. For example, most

#86286 - $15.00 USD Received 10 Aug 2007; revised 14 Sep 2007; accepted 24 Sep 2007; published 25 Sep 2007

integrated fiber oscillators use fiber Bragg gratings (FBGs) to provide the desired feedback; therefore, feedback from spurious Fresnel reflections at component interfaces or from the output facet are undesirable as they could lead to parasitic lasing or reduced slope efficiencies. Fiber amplifiers need to minimize all forms of feedback to maximize the single-pass gain of the injected signal.

The most common source of undesirable fiber feedback is the Fresnel reflection from the fiber facets. Since feedback from the facets is typically wideband due to the relatively weak dispersion of glass over the gain bandwidth of most rare-earth ions, the suppression of feedback, and consequently the reduction of amplified spontaneous emission (ASE) and the avoidance of parasitic lasing, are especially important for low-repetition-rate fiber systems and/or when operating in a spectral region far from the wavelength with maximum gain. This is the case, for example, when building CW or pulsed oscillators or amplifiers operating at the long wavelength tail in Yb^{3+}-doped silica [6, 7]. In these cases, as we discuss in this paper, silicate bonding can be used to dramatically decrease the effective feedback in the double-clad fiber gain medium and mitigate optically induced facet damage.

We propose to accomplish these two goals by bonding optical flats on the output facets of fiber amplifiers as shown in Fig. 1(a). The fiber output mode area expands several orders of magnitude within the flat so that by the time it reaches the optical flat-air interface, the reduced intensity at the interface considerably lowers the probability of contamination-induced catastrophic facet damage. Furthermore, the light that is reflected at the optical flat-air interface expands even further before reaching the fiber core, which results in a dramatic reduction in feedback.

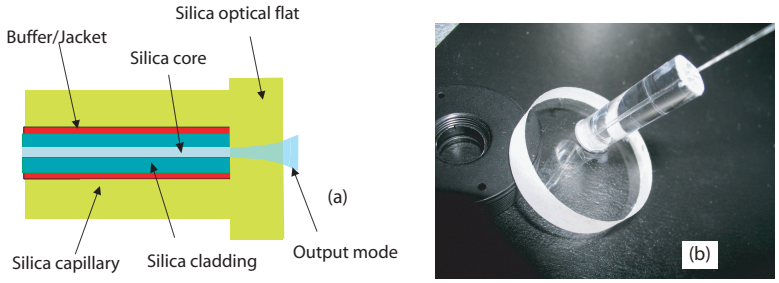

Fig. 1. (a) Illustration of an optical flat bonded to the end of a fiber. The fiber core and the fiber cladding are made of fused silica. The jacket or buffer layer is made of either a polymer or fused silica. (b) Photograph of a double-clad fiber that is silicate bonded to a 1"-diameter optical flat. The fiber has an inner cladding of 250 μm and a low-index acrylate jacket with a diameter of 450 μm. The exterior of the last few centimeters of the fiber's length is epoxied to the inner wall of a thick-walled capillary with a 475-μm inner diameter and a 6-mm outer diameter. The 6-mm diameter capillary is used to provide mechanical support to facilitate polishing and subsequent bonding.

Although silicate-bonded samples have been rigorously studied with respect to their mechanical properties, very little optical characterization of silicate bonding has been reported. To fill this gap, we report measurements of both the optical damage threshold of silicate bonds and the Fresnel reflection from silicate bonds to determine the bonding conditions that will allow us to obtain silicate bonds with optimal optical properties.

2. Background

Silicate bonding (or hydroxy-catalysis bonding) is a low-temperature chemical process, invented by Jason Gwo at Stanford University [8], which is used to bond two flat surfaces to-

#86286 - $15.00 USD Received 10 Aug 2007; revised 14 Sep 2007; accepted 24 Sep 2007; published 25 Sep 2007

gether. The original motivation behind the development of silicate bonding was to find a bonding process that was compatible with the harsh launching conditions in space missions [9]. Silicate bonding was found to be robust and able to withstand a wide range of temperatures. More recently, there has been interest in using silicate bonding to suspend large optical masses for gravitational wave detection. The negligible excess mechanical loss added by the silicate bond allows the process to be compatible with the stringent noise specifications required by this application [10].

The chemistry of the silicate bonding process has been well studied [11]. The first step, hydration and etching, occurs when the two surfaces to be bonded come into contact for the first time with a water-based sodium-silicate solution at the interface. The hydroxide ions etch the surface of the fused silica and release silicate ions as described in the following chemical reaction:

$$SiO_2 + OH^- + 2H_2O \longrightarrow Si(OH)_5^- \tag{1}$$

The consumption of the OH^- ions during the etching process gradually reduces the pH of the solution. Once the pH falls below 11, the silicate ions disassociate to form siloxane chains. This second step, called polymerization, is described by the following two-step chemical reaction:

$$2Si(OH)_5^- \longrightarrow 2Si(OH)_4 + 2(OH)^- \longrightarrow (HO)_3SiOSi(OH)_3 + H_2O + 2(OH)^- \tag{2}$$

The siloxane chains begin to form and lengthen, and a network of these chains grows stronger to begin bonding the two surfaces together. As the bond forms, the final step of dehydration is initiated, during which the water evaporates or enters the bulk of the bonded materials as the bond sets. The duration of this bonding process depends on the bonding conditions and the size of the pieces being bonded.

The exact thickness of the cured bond depends on the bonding conditions, but AFM measurements have shown that the bond thickness of two bonded fused silica pieces using sodium trisilicate solution is on the order of 100 nm [10]. More detailed chemistry of the bonding process can be found in [11]. The bonding procedure that we use is detailed in Appendix A.

3. Preparation of bonded samples

We bonded 200 pieces of high-quality fused silica in pairs to create a total of 100 separate bonded samples. The 200 pieces were cut from a pair of 4" diameter, 20-mm thick optical flats, each of which had a measured peak-to-peak flatness of 60 nm or better over their entire surface. The pieces were cut into rectangular prisms that measured 6 mm x 6 mm x 20 mm. The edges of these prisms were beveled so that the edges of the samples were smooth. The beveling of the samples reduced their bondable area to approximately 30 mm^2.

In creating the 100 bonded samples, we explored a large operating space in bonding conditions encompassing four different concentration values (12.5%, 14.3%, 16.7%, and 20% trisilicate solution volume in total solution volume), five different solution volumes (0.1 μL, 0.2 μL, 0.5 μL, 1.2 μL, and 3.0 μL) and five different curing temperatures (25°C, 90°C, 120°C, 600°C, and 950°C). The concentration-volume-temperature combinations were chosen such that no two samples were bonded identically and all unique combinations of the three parameters were explored (4x5x5=100). More dilute solution concentrations initiate bonding more rapidly due to their lower pH, but the dehydration step requires more time. Lower solution volumes can result in thinner bond interfaces [10], which may result in stronger bonds, but if the volume is too low, the bond interface can contain voids, which can result in decreased bond strength and greater Fresnel reflections. Finally, curing the bond at elevated temperatures can decrease the time it takes for the bond to attain full strength from weeks or months to several days. How-

#86286 - $15.00 USD Received 10 Aug 2007; revised 14 Sep 2007; accepted 24 Sep 2007; published 25 Sep 2007

ever, the stresses incurred during the temperature cycling can offset the advantage of having a quicker turnaround time in manufacturing the bonded samples.

The different temperature curing points were selected to fall within certain important ranges. We wanted to determine the bond properties when cured at room temperature (i.e., 25°C), above room temperature but below the boiling temperature of water (i.e., 90°C), above the boiling point of water but below the thermal damage threshold of most low-index polymers that are used in double-clad fibers (i.e. 120°C), above the thermal damage threshold of polymers but below the boiling point of sodium trisilicate (i.e., 600°C), and above the boiling point of sodium trisilicate but below the melting point of fused silica (i.e., 950°C).

Only 16 of the 200 samples failed to bond properly. It should be noted that of these 8 pairs of bonded samples that did not survive the bonding process, 7 were cured at high temperatures of either 600°C or 950°C. This high overall yield of 92% (with a yield of 98.3% for samples cured at temperatures of 120°C or lower) indicates that silicate bonding can be suitable for commercial processes. In the remainder of this paper, we will measure the feedback and optical damage properties of these different bonding conditions to determine the best bonding procedure for our application.

4. Pump power handling of double-clad silicate-bonded fibers

The outer cladding of many silica double-clad fibers is constructed from a low-index polymer to allow for the creation of a large numerical aperture (NA) for the pump in the inner cladding. During polishing, this soft polymer is not uniformly removed; instead the polymer is removed via microscopic tearing due to the elastic nature of the material. This results in a small valley between the silica inner cladding and the silica capillary that extends around the perimeter of the fiber. This valley also includes the cured UV epoxy, which is also softer and more elastic than the fused silica. This discontinuity in the fiber cross-section, and the possible void between the end of the polymer and the bonded flat at the end of the fiber, could result in excess pump scattering and increased pump feedback, which could damage the polymer or epoxy and limit the pump power handling of the fiber.

To determine how much pump power can be handled at this silicate bond for a typical double-clad fiber, we silicate bonded a double-clad passive fiber that had an inner cladding of 250 μm and a low-index acrylate jacket with a diameter of 450 μm. The 3-cm long, thick-walled capillary had a 475-μm inner diameter and a 6-mm outer diameter, with the UV epoxy filling the volume between the fiber and the capillary inner wall. The other end of the fiber was cleaved. We inserted this bonded fiber sample into an optical setup. The cleaved fiber end was aligned to the output of a fiber-pigtailed laser-diode stack and the amount of power coupled into the inner cladding of the passive fiber was slowly increased while the polymer jacket and UV epoxy at the silicate-bond interface was closely monitored for the onset of damage. No damage was observed over nearly ten hours with 50 W of pump power at the silicate bond interface. However, when we increased the coupled pump power to 60 W, thermally-induced damage resulted in the polymer material after 30 minutes, at which point the pump intensity was approximately 120 kW/cm^2.

Well-designed high-power cladding-pumped fiber lasers and amplifiers typically have less than 10% of their coupled power unabsorbed. Thus, if the pump power is not coupled through the silicate-bonded end (i.e., the output is extracted from the opposite end of the fiber from the pump-coupling fiber end), silicate bonding of an optical flat to the output end of a double-clad fiber amplifier with a polymer outer cladding with similar dimensions should allow for coupled pump powers of at least 500 W. All-silica fibers should handle considerably higher powers since the UV epoxy should see considerably lower pump power than the outer cladding.

#86286 - $15.00 USD Received 10 Aug 2007; revised 14 Sep 2007; accepted 24 Sep 2007; published 25 Sep 2007

5. Facet damage issues

To help resolve the issue of facet damage, the technique of fusion splicing coreless end caps to increase the spot size at the silica-air interface is widely used in high-power fiber amplifiers to reduce the intensity at the silica-air interface (see Fig. 2) [12]. These core-less end caps are solid fibers (i.e., the first and only cladding is formed by the surrounding air) that are spliced to the output end of the fiber amplifier and then polished down to an appropriate length. The splices are strongest when the diameter of the end cap is matched to the diameter of the output gain fiber, which also simplifies the polishing process. Thus, the beam radius can only be expanded to about a third of the fiber diameter if aperture effects are to be avoided.

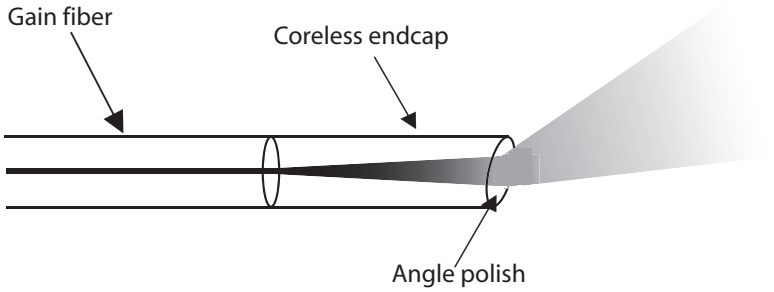

Fig. 2. Coreless end cap spliced to the gain fiber. The end cap is polished at an angle to suppress feedback. The polish angle and the angle of the free-space output beam with respect to the fiber axis are exaggerated for clarity.

This limitation can be circumvented by using a larger diameter fiber, but the increased mechanical rigidity of the fiber would increase the minimum allowable bend radius of the fiber. This could in turn negatively impact the mode quality for fiber lasers that employ bending losses to improve the spatial beam quality of the output. Furthermore, the larger bend radius would increase the footprint of the system (which even affects fiber systems that do not use bending losses to control beam quality). In addition, splicing end caps becomes more challenging as the fiber diameter is increased due to the increased arc energy that is required to melt the glass.

A second option would be to use an adiabatic taper to expand the mode. However, it is difficult in practice to adiabatically increase the mode size by orders of magnitude without significant loss or the appearance of higher order modes. For this reason, adiabatic tapers are rarely used today with high-power fiber sources unless the required mode expansion is quite small.

A third option would be the silicate bonding of an optical flat to the output fiber. The diameter and thickness of the flat can be chosen by the user to decrease the output intensity at the silica-air interface by many orders of magnitude. In addition, since silicate bonding can be done at room temperature, this process is scalable to fibers with large diameters.

Ideally, these three approaches, which all work by moving the silica-air interface from the high-intensity output of the fiber to a point where the mode is much larger and the intensity much weaker, would allow for the damage threshold of the output fiber end to be the same as the bulk by eliminating surface states and submicroscopic surface defects. However, even if these approaches do not increase the damage threshold of the fiber end to the bulk value, the elimination of contaminants alone at the high-intensity output end of the fiber can increase the safe and reliable maximum operating power of the source by several orders of magnitude (depending on the operating environment).

#86286 - $15.00 USD Received 10 Aug 2007; revised 14 Sep 2007; accepted 24 Sep 2007; published 25 Sep 2007

5.1. *Derivation of intensity reduction using bonded flats*

We calculated the achievable reduction in intensity at the silica-air interface for different fibers using either coreless end caps or silicate bonded flats. Three fiber core sizes were modeled: (1) Standard single-mode fibers at 1-μm operating wavelength with 5-μm diameter core and 6.8-μm mode field diameter, (2) The largest core diameter attainable for single-mode operation at 1.06 μm with 0.06 NA, and (3) The largest core diameter attainable for single-mode operation at 1.06 μm with 0.02 NA. The mode-field radius, w, for the LP_{01} fundamental mode for a fiber with a given core radius a and V-number is given approximately by [13]:

$$w = a(0.65 + 1.619V^{-1.5} + 2.879V^{-6}) \tag{3}$$

where $V = (2\pi aNA)/\lambda$. An operating wavelength of 1064 nm and an effective index of refraction of 1.45 were assumed. The inner cladding was varied for each of the fiber mode field diameters as shown. The total diameter of the fiber, and therefore the diameter of the coreless end cap, was set to be 3.5 times to the inner cladding diameter. This ratio is consistent with the upper range for the ratio of inner cladding to fiber diameter for commercial active fibers. The length of the coreless end cap was chosen such that the radius of the mode exiting the end cap was a factor of π smaller than the end cap diameter. This limit to the end cap length is necessary to prevent distortion to the beam profile due to aperture-induced diffraction [14]. The length of the silicate bonded 1"-diameter flat was fixed at 2 cm for all cases, which is a standard thickness for commercial optical flats.

The results of our calculation, shown in Fig. 3, demonstrate that for all mode-field diameters, the silicate-bonded flat exhibits significant reduction in the silica-air intensity over the coreless end cap. This is because the diameter of the silicate bonded flat is not restricted by the outer diameter of the fiber. This would allow these fiber systems to be used in industrial applications, where the environment may not be well controlled, without the need for a hermetically-sealed housing. Furthermore, the intensity reduction from the silicate bond is independent of the inner cladding size, which would allow the use of large mode area (LMA) fibers with small inner claddings for highly efficient pump absorption.

5.2. *Damage threshold of silicate bond*

However, this enhanced intensity reduction assumes that the silicate bond itself has a comparable damage threshold to the silica-air interface. To our knowledge, the optical-damage threshold of silicate bonds has never been carefully measured. It is possible that the bonding process leaves microscopic voids that can initiate damage. Alternately, the siloxane chains that form the bulk of the bond could have measurable absorption at 1064 nm that can cause thermally induced damage. We tried to measure the CW damage threshold of the silicate bonds with a 40-W diffraction-limited solid-state laser, but none of the silicate-bonded samples damaged, even with incident beam diameters to the bond as small as 20 μm. Therefore, we opted to measure the pulsed damage threshold of the bond instead.

We measured the damage statistics of the silicate bonded samples at two different pulse widths. The first damage measurements were made with $\sim$1-μs-long pulses. These pulses were considerably longer than the 10-ns Q-switched pulses that are typically used to measure the damage properties of optical materials. The results from this test can be used to shed some light on the CW damage threshold of the silicate bond. The samples that survived the 1-μs pulse test were subsequently subjected to the standard Q-switched damage threshold measurement.

The experimental setup to generate high-energy 1-μs pulses is shown in Fig. 4. The system consisted of a single-frequency, 600-mW Nd:YAG NPRO operating at 1064 nm, which was modulated and amplified through a series of Nd:YAG laser rods. The polarized output of the system was then focused with a lens on the silicate bond. The power incident on the bond was

#86286 - $15.00 USD Received 10 Aug 2007; revised 14 Sep 2007; accepted 24 Sep 2007; published 25 Sep 2007

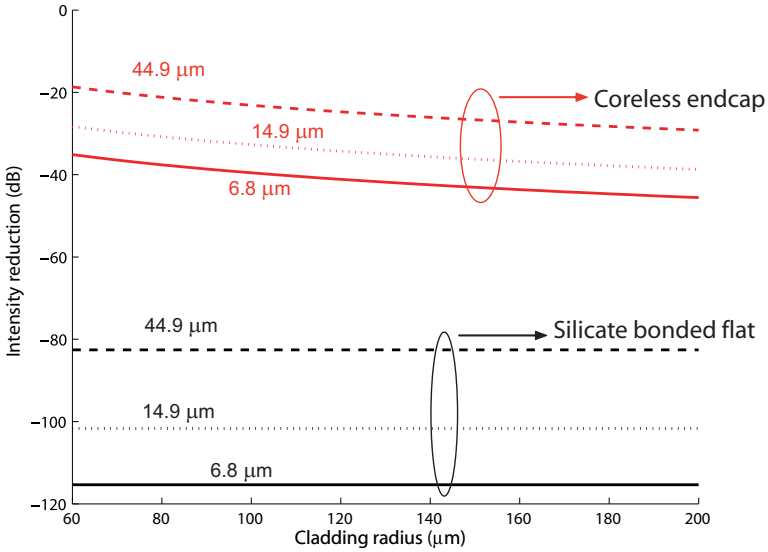

Fig. 3. Intensity reduction at silica-air interface for different fiber end treatments. The reduction is plotted for fibers with mode field diameters as shown. The operating wavelength is 1064 nm.

controlled with a half-wave plate and a polarizing beam splitter. The output pulse shape in the time domain was controlled with an arbitrary function generator driving the AOM to ensure that there were no satellite pulses, that the pulse shape was repeatable, and that the shot-to-shot fluctuations in energy were less than 5%.

The incident pulse had a FWHM pulse width of 880 ns and no satellite pulses were observed. A maximum incident energy of 100 mJ was measured at the bond. The spot was focused to a $1/e^2$-intensity diameter $2w_0$ of 210 μm and 170 μm for the horizontal and vertical dimensions, respectively. This diameter was chosen for two reasons. First, the Rayleigh length $z_r = \pi n w_0^2/\lambda$ of this beam was large enough that we did not have to position the sample along the beam's propagation direction with a high degree of accuracy to obtain similar fluences incident on the silicate bond from sample to sample. Second, the large waist of the beam allowed the sampling of the damage threshold of a bonded area considerably larger than the mode field area of a gain fiber (even for LMA fibers with mode field diameters of tens of micrometers). This allowed us to test the uniformity of the damage threshold over a larger area than needed, which gave us information on the probable yield of the bond. Given the available energy and measured spot size, the silicate bonds were subjected to a maximum peak power of 435 MW/cm^2 and a maximum fluence of 357 J/cm^2.

The surface damage fluence of fused silica, F_{dam}, at 1 μm is given empirically by [15]:

$$F_{dam} = 22\Delta\tau^{0.4} \tag{4}$$

where $\Delta\tau$ is the FWHM pulse width of the laser in nanoseconds and F_{dam} has units of J/cm^2. The damage coefficient (22) in Equation (4) depends greatly on surface preparation and has been measured to be as high as 34 [16]. For our pulse width of 880 ns, F_{dam} equals 331 J/cm^2 if we assume a damage coefficient of 22.

Each sample was individually inserted into a holder and the incident pulse energy was slowly increased. The onset of damage was determined when either an increase in scattered light was observed or a decrease in pulse energy transmission was measured, as shown in Fig. 4. If the

#86286 - $15.00 USD Received 10 Aug 2007; revised 14 Sep 2007; accepted 24 Sep 2007; published 25 Sep 2007

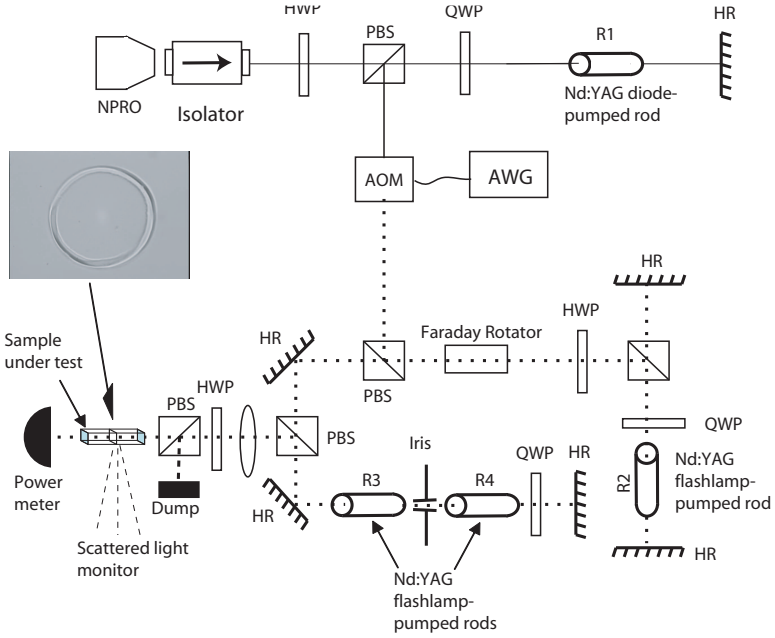

Fig. 4. Experimental setup for measuring microsecond damage threshold of silicate bond. The laser system produces 100-mJ, 880-ns pulses at 1064 nm. AOM: acousto-optic modulator, HWP: half-wave plate, QWP: quarter-wave plate, PBS: polarizing beamsplitter, AWG: arbitrary waveform generator, HR: high reflector. Included is a photograph of the damage induced by the microsecond pulse in one of the samples. The diameter of the outer circle shown is approximately 420 μm.

sample remained undamaged at the maximum available energy of 100 mJ, the sample was subjected to approximately 400 pulses at this maximum fluence. If the onset of damage was still not observed, we slowly decreased the fluence to zero and removed the sample for further testing with the Q-switched laser. The inset in Fig. 4 shows a picture of the bond interface for one of the damaged samples using a microscope. The damage spot was similar in dimension and shape to those observed in polished fused silica surfaces [16]. The damage statistics with the microsecond-pulses for the samples for the different solution concentrations, the different solution volumes, and the different curing temperatures, are plotted in Fig. 5. For each data point in the three subplots of Fig. 5, the bonding parameter on the x-axis was fixed and all samples with that fixed parameter were used, regardless of the other two bonding parameters (e.g., for the data point for 0.5 μL, the data for all samples with 0.5 μL were used, regardless of their solution concentration or their curing temperature). Of the 92 samples, 32 samples were damaged by the microsecond pulses. The average damage energy was 64.8 mJ and the median was 58 mJ.

The concentration group with the smallest fraction of damaged samples was 16.7% by volume of sodium trisilicate (see Fig. 5(a)). With the exception of the solution volume group of 0.5 μL, all volumes yielded about the same fraction of damaged samples (see Fig. 5(b)). As we see in the subsequent section, this high damage probability for 0.5 μL is most likely a statistical artifact. Hence, solution volume appears to have a weak effect on the damage threshold of the bond. More than 75% of the samples cured at 600°C suffered damage (see Fig. 5(c)). Otherwise, the damage statistics did not seem to overly depend on the temperature at which the bond was cured.

#86286 - $15.00 USD Received 10 Aug 2007; revised 14 Sep 2007; accepted 24 Sep 2007; published 25 Sep 2007

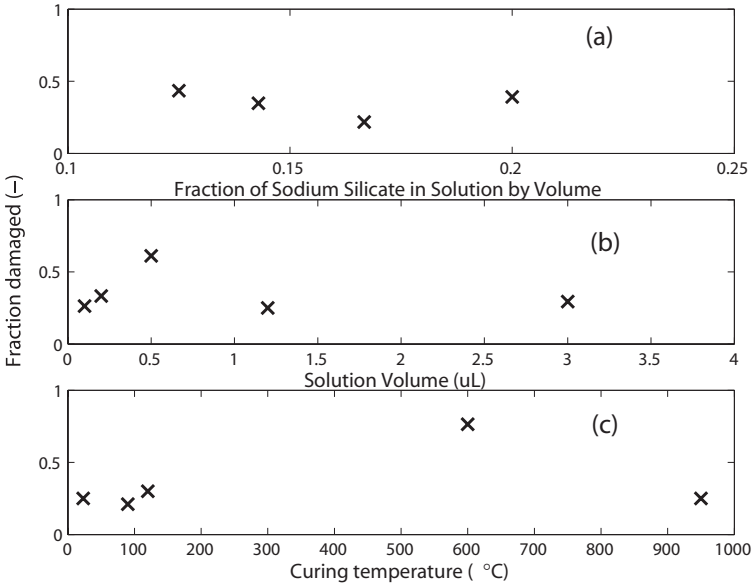

Fig. 5. Fraction of damaged samples with microsecond incident pulses for different (a) solution concentrations (b) solution volumes and (c) curing temperatures.

We measured the damage threshold of the silicate-bonded samples on the nanosecond time scale using a commercial Q-switched Nd:YAG rod laser (Quanta-Ray model DCR) capable of producing several hundred millijoules of energy. We operated the laser with a 25-ns FWHM pulse width at a pulse repetition frequency of 10 Hz. We focused its output beam onto the bond of the silicate-bonded samples with a $1/e^2$ spot diameter of 250 μm. This laser spot was chosen to be slightly larger than the size used for the microsecond-damage measurements because the output from the Q-switched laser was not diffraction limited. Once again, the long Rayleigh range of loosely focused beam obviated the need to align the sample carefully in *z*. The onset of damage was easily observed by the large decrease in transmitted energy. Pulses following the initial damaging pulse would extend the damage backwards from the bond along the propagation path of the beam towards the laser, until a channel was drilled along the length of the fused silica sample that stretched from the silicate bond to the entrance of the sample.

For several samples, the AR-coated entrance or exit face of the silicate-bonded sample damaged before the bond. This was presumably due to some surface contamination, and these samples were not included in our analysis. Figure 6 shows the median damage thresholds for the various bonding conditions. The solution concentration that yielded the highest median optical damage threshold was 20% by volume of sodium trisilicate (see Fig. 6(a)). In general, the median damage threshold appears to increase with increasing solution concentration. Figure 6(b) shows that, with the exception of the solution volume group of 0.5 μL, there appears to be very little dependence of the nanosecond optical damage threshold on solution volume (which is consistent with our data from the microsecond optical damage tests). The median damage threshold is likely higher for the 0.5 μL volume group because the "weaker samples" were taken out by the microsecond damage test, which skewed the median upward.

Finally, it appears that the nanosecond optical damage threshold increases with curing temperature up to a point (see Fig. 6(c)). At the very high temperatures of 600°C and 950°C, the optical damage threshold appears to have been substantially reduced. The optimum temperature

#86286 - $15.00 USD Received 10 Aug 2007; revised 14 Sep 2007; accepted 24 Sep 2007; published 25 Sep 2007

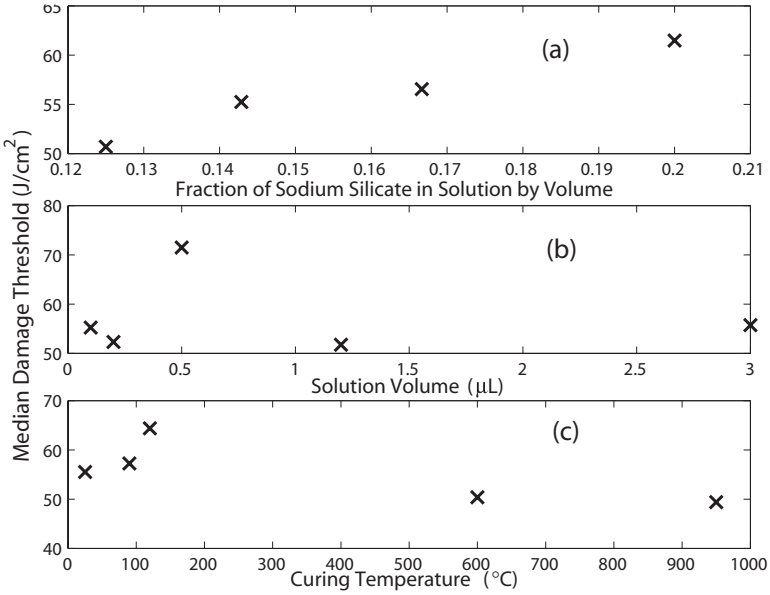

Fig. 6. Median Q-switched damage threshold for silicate-bonded samples with different (a) solution concentrations (b) solution volumes and (c) curing temperatures.

appears to be 120°C, which also exhibited the best performance in the microsecond-damage tests. Thus, the damage threshold of silicate bonds can approach the damage threshold of an uncontaminated, well-prepared fused-silica surface. Therefore, we conclude that silicate bonding can be used to mitigate the appearance of facet damage in high-power fiber sources.

6. Feedback minimization

As stated in Section 1, the minimization of feedback into the gain medium due to the Fresnel reflection from the fiber facets is essential in low-repetition rate pulsed amplifier systems and when operating at a wavelength far from the peak-gain wavelength. The amount of feedback can be decreased substantially by angling the fiber facet appropriately such that the reflected beam is not coupled back into the core. We can derive the expression for the amount of feedback in a fiber due to Fresnel reflection for a given facet angle. We can then extend this expression to determine the level of effective feedback seen at the facet of a double-clad fiber, which will allow us to calculate the feedback in double-clad fibers with the different facet terminations.

6.1. Derivation of effective feedback from double-clad fiber facets

We begin with the expression giving the amount of power coupled into a single-mode fiber with circular symmetry from a free-space incident beam, as illustrated in Fig. 7(a) [17]:

$$T = \frac{4w_{fiber}^2 w_x w_y}{(w_x^2 + w_{fiber}^2)(w_y^2 + w_{fiber}^2)} e^{-\frac{2\pi^2 w_{fiber}^2}{\lambda^2}\left[\frac{w_x^2 \sin^2\theta_x}{w_x^2 + w_{fiber}^2} + \frac{w_y^2 \sin^2\theta_y}{w_y^2 + w_{fiber}^2}\right]} \tag{5}$$

where w_{fiber} is the mode-field radius in the fiber, w_x and w_y are the horizontal and vertical mode-field radii for the incoming beam, θ_x and θ_y are the horizontal and vertical angular tilts of the free-space incoming beam with respect to the fiber axis, respectively, and λ is the operating

#86286 - $15.00 USD Received 10 Aug 2007; revised 14 Sep 2007; accepted 24 Sep 2007; published 25 Sep 2007

wavelength of the incident beam in vacuum. The NA of the fiber is chosen such that the fiber is close to cutoff and all higher order modes are very strongly attenuated. We assume that there is no Fresnel loss at the entrance to the fiber (i.e., the free-space medium has the same refractive index as the fiber).

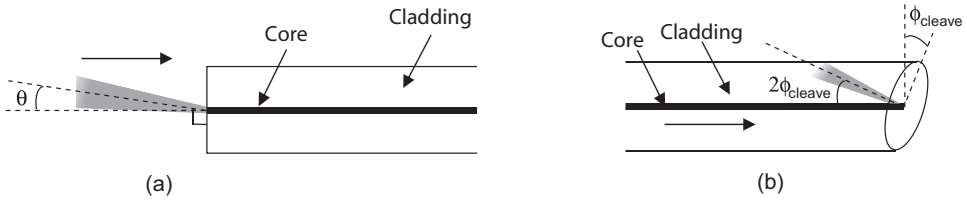

Fig. 7. (a) Coupling of a free-space off-axis mode-matched beam to a single-mode fiber. (b) Feedback from the Fresnel reflection in a fiber with an angled output facet.

To simplify Eq. (5), we make two assumptions. First, we assume that the free-space beam is circular and mode-matched to the fiber mode (i.e., $w_x = w_y = w_{fiber} = w$). Second, we assume that the tilt is only in the vertical direction (i.e., θ_x = 0 and $\theta_y = \theta$). The second assumption can be made without loss of generality since the fiber has circular symmetry. Under these conditions, Equation (5) reduces to:

$$T = e^{-\frac{\pi^2 w^2 \sin^2\theta}{\lambda^2}} \tag{6}$$

For a fiber with an angled output facet, the angle of the reflected beam with respect to the fiber axis inside the fiber is identical to the angle θ resulting from an incoming free-space with the angular tilt given by Snell's Law, as shown in Fig. 7(b):

$$\theta = \sin^{-1}(n\sin(2\phi_{cleave})) \tag{7}$$

where ϕ_{cleave} is the angle of the normal of the output fiber facet with respect to the fiber axis and is aligned in the same direction as the tilt of the input beam. n is the index of refraction of the fiber. Equation (7) can be substituted into Equation (6) and the Fresnel reflection at the fiber-air interface can be incorporated to derive the feedback, F, resulting from an angled facet:

$$F = R(\phi_{cleave})e^{-\frac{\pi^2 w^2 [n\sin(2\phi_{cleave})]^2}{\lambda^2}} \tag{8}$$

where R is the angle-dependent Fresnel reflection from the angled output facet, given by:

$$R(\theta) = \eta \left| \frac{\cos\theta - \sqrt{\frac{1}{n^2} - \sin^2\theta}}{\cos\theta + \sqrt{\frac{1}{n^2} - \sin^2\theta}} \right|^2 + (1-\eta) \left| \frac{-\frac{1}{n^2}\cos\theta + \sqrt{\frac{1}{n^2} - \sin^2\theta}}{\frac{1}{n^2}\cos\theta + \sqrt{\frac{1}{n^2} - \sin^2\theta}} \right|^2 \tag{9}$$

where η is the fraction of the incident power in the s-polarization. In the case of internal reflection (i.e., entering a medium with a lower refractive index), the power reflectivity is greater for the s-polarization than the p-polarization. Thus, for a worst-case scenario for the feedback, we will assume that $\eta = 1$.

By using Eqs. (8) and (9), we can calculate the feedback versus facet angle for several mode sizes, as shown in Fig. 8. As before, we modeled single-mode fibers with three different mode field diameters, namely 6.8-μm, 14.9-μm, and 44.9-μm, as used in the simulation shown on Fig. 3. It is clear that the smaller NAs of the larger mode area fibers allow for significantly

#86286 - $15.00 USD Received 10 Aug 2007; revised 14 Sep 2007; accepted 24 Sep 2007; published 25 Sep 2007

decreased feedback. For facet angles above 8°, stimulated Rayleigh scattering will likely place a lower limit on the lowest achievable feedback attainable in a fiber system [18] for all NAs. Since the total amount of Rayleigh scattering increases with fiber length, shorter fiber lengths will have lower feedback. In addition, the Rayleigh scattering per unit length can be decreased by lowering the NA of the core.

We also modeled optical feedback from double-clad fibers with (1) an angled facet, (2) a coreless endcap spliced at the output, and (3) an optical flat bonded to the output of the fiber. Equation (8) assumes the light reflected from the fiber facet that is not coupled into the core is scattered away. This assumption, while valid for single-clad fibers, is not justified in double-clad fibers, where the large NA of the inner cladding can easily guide the uncoupled radiation. The light coupled in the inner cladding will interact periodically with the active core and its dopant ions, resulting in a higher level of effective feedback. The exact level of interaction of the inner cladding light with the core is impossible to predict without knowing the degree of excitation of each cladding mode. However, to model the effective feedback from the Fresnel reflection to first order, we can assume that the light guided in the inner cladding interacts with the core according to the ratio of the core to cladding area.

The calculated results for these three situations, determined for fibers with the same mode field diameters as in Fig. 8, are shown in Fig. 9. The inner cladding was varied for each of the fiber mode field diameters as shown. The total diameter of the fiber (and therefore the diameter of the coreless end cap) was set to be 3.5 times the inner-cladding diameter as in Section 5. The length of the coreless end cap was constrained to avoid the appearance of aperture-induced diffraction. The angle of the cleave and the polished end-facet of the coreless end cap were set to 8°. The length of the silicate bonded flat was fixed at 2 cm for all cases, which is a standard thickness for commercial optical flats.

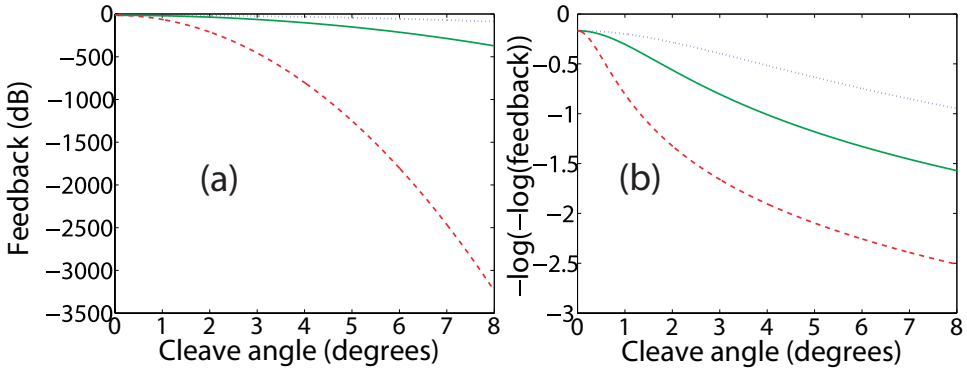

Fig. 8. Feedback resulting from angled facet. The feedback is plotted for fibers with mode field diameters of 6.8 μm (dotted, blue), 14.9 μm (solid, green) 44.9 μm (dashed, red). 8 degrees is the standard facet angle for angle-polished standard single-mode fibers. Plot (a) illustrates the feedback in dB. For clarity, plot (b) plots the negative logarithm of the negative logarithm of Equation (8).

Although we showed in Fig. 8 that single-mode fibers with large cores and resultant small NAs have low direct coupling into the core from an angled cleave, examination of the data in Fig. 9 demonstrates that the large mode field areas can have significant amounts of effective feedback in double-clad fibers when angle-cleaved. The use of a coreless end cap dramatically reduces the effective feedback. However, the limit to the end cap length still permits a level of feedback that would be troublesome in low-gain wavelength systems by providing sufficient

#86286 - $15.00 USD Received 10 Aug 2007; revised 14 Sep 2007; accepted 24 Sep 2007; published 25 Sep 2007

feedback for ASE growth.

The bonding of a 2-cm silicate bonded flat reduces the feedback for even the largest mode-field area simulated to less than -100 dB (see Fig. 9). This is likely well below the stimulated Rayleigh scattering-induced lower bound for feedback for gain fibers of reasonable length. Furthermore, since the feedback level for the silicate-bonded case is almost completely independent of the inner cladding radius, large mode-field diameters can be used in conjunction with small inner cladding radii for higher pump absorption per unit length to allow for the construction of shorter devices. This reduction device length will permit higher powers to be obtained before the onset of nonlinear optical effects, provided that the increased thermal load can be managed.

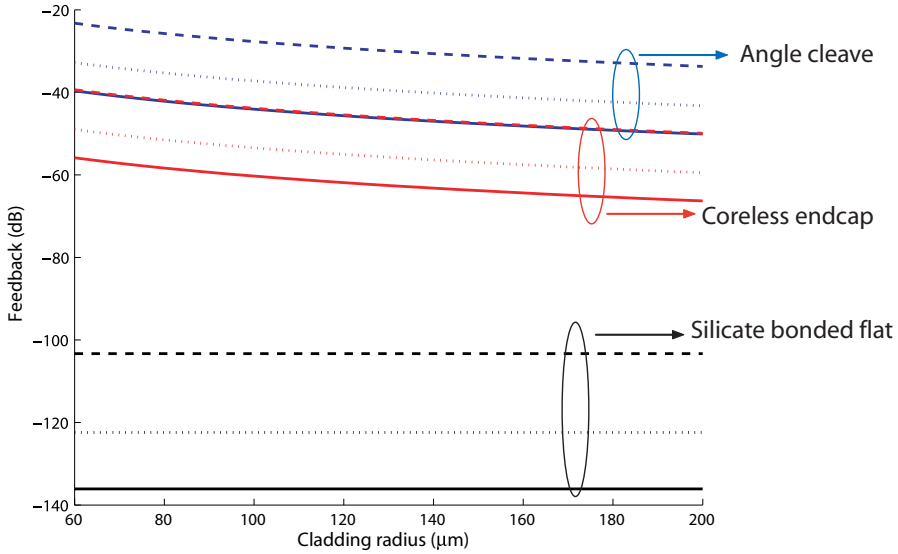

Fig. 9. Effective feedback for various fiber termination schemes for fiber with mode field diameters of 6.8 μm (solid), 15.9 μm (dotted) and 44.9 μm (dashed) versus inner cladding radius. The effective feedback curve for the 6.8 μm angle-cleaved fiber lies directly atop the curve for the 44.9-μm coreless end cap. The largest inner cladding radius plotted corresponds to a total fiber diameter of 1.4 mm.

The curves shown in Fig. 9 for the coreless end cap and the silicate-bonded flat assume that there is no Fresnel reflection between the splice and bond interface, respectively. This is reasonable since it is straightforward to find a glass that matches the effective index of the guided mode in the core to within 0.0015 or better over a 150-nm wavelength range. This index mismatch would give a Fresnel reflection of -65 dB. Since a splice fuses the two materials together, the coreless end cap would have very low Fresnel losses at the splice interface provided the end cap material is well-chosen. On the other hand, the reflection from a silicate bond has never been measured. This level of feedback depends both on the index of refraction of the bonding material and the thickness of the bond. If the Fresnel reflection of the silicate bond is high, then the effectiveness of this approach to reduce feedback would be compromised.

#86286 - $15.00 USD Received 10 Aug 2007; revised 14 Sep 2007; accepted 24 Sep 2007; published 25 Sep 2007

6.2. *Measurement of Fresnel reflection from silicate bond*

We measured the Fresnel reflection from a silicate bond under different bonding conditions using a 10-W Nd:YAG 1064-nm mode-locked laser, as shown in Fig. 10. It should be noted that these measurements were made before the optical damage characterization described in Section 5. The mode-locked laser pulse was reflected by three interfaces: the silica-air interface at the entrance of the bonded sample, the silicate-bond interface at the center of the sample, and the silica-air interface at the exit of the bonded sample. The reflection off the bond was temporally separated from the reflection off the end-facets by the amount of time it took the laser pulse to make a roundtrip through one of the 2-cm-thick fused-silica samples that were bonded. The group of three reflections were observed with a fast sampling oscilloscope. The relative magnitude of the second peak compared to the first and third peaks determines the reflection off the silicate bond. The reflections from each of the interfaces are equally spaced by:

$$\Delta\tau = \frac{2nL}{c} \tag{10}$$

where L is the length of one of the samples that was cut from the optical flat (measured to be 2 cm) and n is the index of refraction of fused silica (assumed to be 1.45). Thus, the reflected pulses are separated by 207 ps. The mode-locked laser repetition rate is 80 MHz, so the spacing between successive ∼400-ps triplets of reflection peaks is 12.5 ns, which ensures that no overlap occurs between successive triplets. We determined that temporally resolving the reflected pulses gives better sensitivity than trying to resolve the reflected pulses spatially by entering the sample at an off-normal angle.

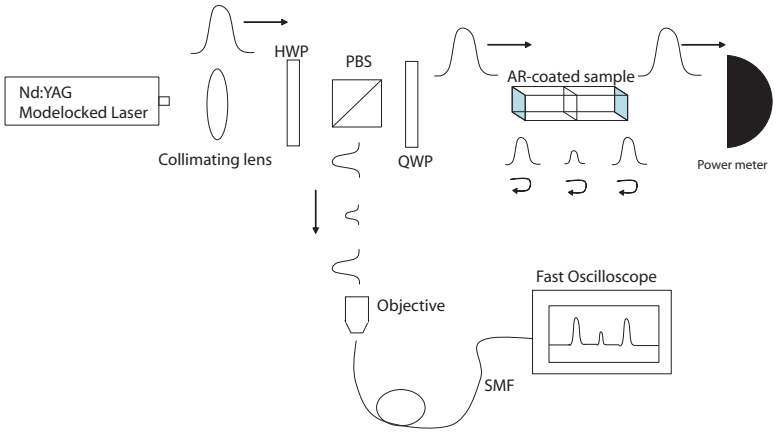

Fig. 10. Experimental setup to measure Fresnel reflections from silicate bonds. The pulse width of the 10-W Nd:YAG mode-locked laser is 3 ps, which is considerably shorter than the 20-ps resolution of our oscilloscope.

Reflection traces of two samples as measured by the sampling oscilloscope are shown in Fig. 11(a). These traces show two large peaks corresponding to the Fresnel reflection from both the front and rear silica-air surfaces of the bonded sample. A reflection peak located symmetrically between these two large peaks would indicate the amount of Fresnel reflection from the silicate bond. The sampling oscilloscope has a risetime of 7 ps when the integrated photodiode is used. However, the ringing from the photodiode signal limits the sensitivity of the bond measurement. Specifically, although the oscilloscope is equipped with a 14-bit D/A converter, ringing from the generated reflection signal off the silica-air entrance end of the bonded samples limited the

#86286 - $15.00 USD Received 10 Aug 2007; revised 14 Sep 2007; accepted 24 Sep 2007; published 25 Sep 2007

minimum detectable reflection from the silicate bond to approximately $1/500^{th}$ of the front-facet reflected signal, even when multiple acquisitions were averaged by the oscilloscope, as illustrated in 11(b). For our bonded fused-silica samples, this would limit our sensitivity in measuring the Fresnel reflection to approximately -40 dB.

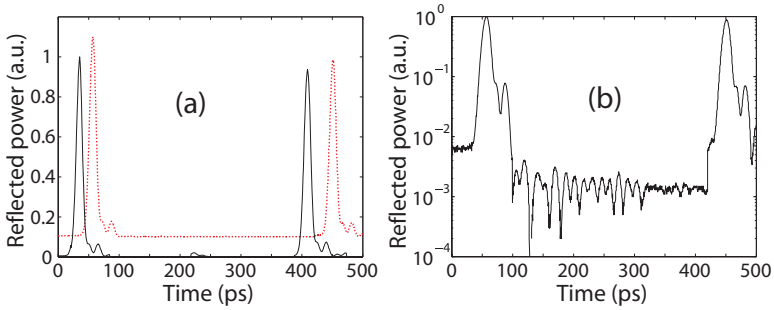

Fig. 11. Traces of the reflections from various interfaces in silicate bonded samples. Plot (a) shows the traces on a linear scale for a sample with a measurable bond reflection (solid, black) and for a sample with a bond reflection below the detectable limit of the experimental setup (dotted, red). Plot (b) shows the trace for the sample with the undetectable bond reflection on a logarithmic scale.

To increase this sensitivity, we had a high-quality low-temperature anti-reflection coating applied to both ends of all samples *after* they were bonded together. The coating run was made at 90°C. The reflection of the coated faces of the samples at the test wavelength of 1064 nm was measured to be approximately 0.025% at normal incidence. This low reflection allowed bond reflections as low as -63 dB to be detected. The beam was collimated at the sample with a 1-mm diameter. The small divergence angle of this large collimated beam minimized the reflection from the narrowband AR-coating at the entrance and exit facets, and ensured that the coupling efficiency to the fiber-coupled photodetector could be made virtually identical for each of the three reflected beams. Each sample was carefully placed in a custom holder, then aligned so that the reflection peaks from both ends of the bonded sample had similar amplitudes. We were unable to observe any scattering off the bond using an infrared imager, even with the maximum power of the mode-locked laser incident on the samples.

We measured the reflection from the silicate bond for all of the bonded samples. The reflection statistics for the samples for the different solution concentrations, the different solution volumes and the different curing temperatures, are shown in Fig. 12. We first note that the measured reflection values from all sample groups were very low, with a maximum median reflection of -46 dB. We observe that the solutions with a higher concentration of sodium trisilicate have a lower reflection. This indicates that the time for polymerization to begin is perhaps not as critical as minimizing the duration of the final dehydration step.

Figure 12(b) indicates that larger solution volumes minimize the reflection off the bond. The 3-μL volume group, which yielded the lowest median reflection, corresponds to 0.10 μL/mm^2 of solution applied per bonded area. This value was somewhat unexpected since it is several times larger than the volume of solution used per bonded surface area previously reported by other research groups [10, 19]. However, these prior works were only concerned with the mechanical properties of the bond, so the small voids in the bond that they observed were probably not important so long as the overall strength of the bond was maximized and the mechanical losses were small. For the purpose of feedback minimization, however, these voids are undesirable, and a slightly thicker silicate bond could be tolerated so long as the strength of the bond is not severely compromised.

#86286 - $15.00 USD Received 10 Aug 2007; revised 14 Sep 2007; accepted 24 Sep 2007; published 25 Sep 2007

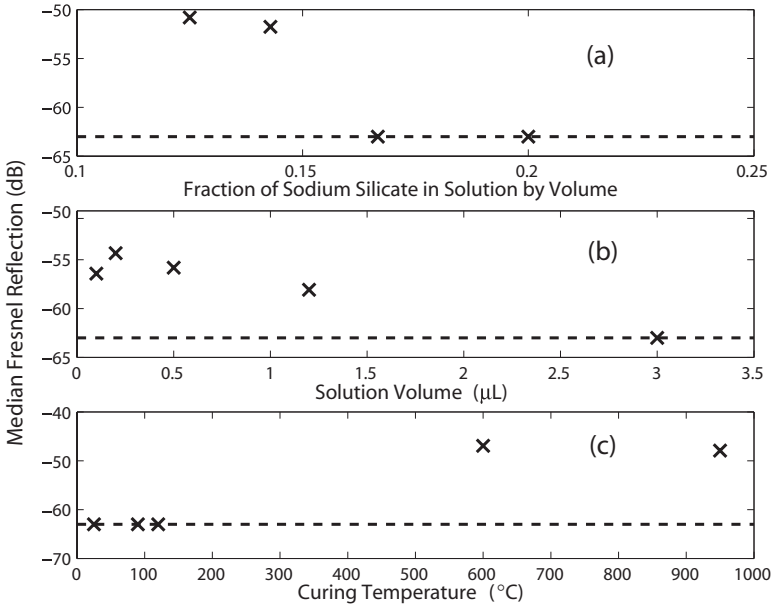

Fig. 12. Measured reflection off of silicate bond versus different (a) solution concentrations (b) solution volumes and (c) curing temperatures. The median reflection value for each group is plotted. The dotted line indicates the sensitivity of the measurement.

Finally, Fig. 12(c) illustrates that the use of lower curing temperatures results in lower bond reflections. The two highest temperature curing points may have overly accelerated dehydration and hence caused voids to appear in the bond interface, and hence increased the reflection off the bond. The 120°C curing temperature is interesting because that is the maximum operating temperature of the polymer outer claddings and jackets used in many double-clad fibers. This temperature could represent the optimum temperature to speed up the dehydration process without leading to a measurable increase in Fresnel reflection from the bond or deterioration of the fiber jacket. It should be noted that the samples cured at 25°C samples were exposed to higher temperatures during the 90°C anti-reflection coating run. However, the duration of the coating run was only a few hours and the coating was applied more than a month after the samples were bonded.

These results show that a silicate bond can be used to significantly reduce the effective feedback at the output facets of double-clad fibers. This can significantly improve the performance of fiber lasers and amplifiers operating at wavelengths far from the maximum gain. The feedback of -63 dB would be attained if the optical flat were bonded to a fiber that was polished such that the normal of the facet is parallel to the optical axis of the fiber. The feedback would be even lower if the flat were bonded to an angle-polished fiber. For example, the feedback for the three different double-clad fibers simulated in Fig. 9, each with flats silicate bonded to 8° angle-polished facets, would be approximately 50 dB below the plotted facet feedback from simply angle-cleaving the three fibers at 8°. In addition, since the best silicate bonds were obtained by low-temperature curing (less than 120°C), an anti-reflection (AR) coating can easily be applied to one side of an unbonded optical flat, then the uncoated side can be bonded to the fiber to further reduce feedback and enhance the output power by eliminating the 4% fused silica-air Fresnel reflection.

In the future, we plan on determining the bond thicknesses of the silicate bonded samples

#86286 - $15.00 USD Received 10 Aug 2007; revised 14 Sep 2007; accepted 24 Sep 2007; published 25 Sep 2007

with an AFM. With the bond thickness and the measured reflection, we will be able to calculate the difference in refractive index of the bond material from the bulk fused silica samples being bonded.

7. Mechanical strength of silicate bonds

Since we are not using silicate bonding for its traditional application in optics suspension, obtaining high mechanical strength is not overly important. However, the bond should be strong enough to withstand shocks experienced in an industrial environment or during shipping.

We tested the shear strength of three samples that were randomly chosen from the samples that survived the microsecond-pulse damage test and were not subjected to the Q-switched-pulse damage test. Our setup to measure shear strength is shown schematically in Fig. 13(a). The fixed end of the sample was held down to the table either manually or with a clamp. The cable suspending the weights was placed as close to the bond as possible on the free end to minimize the applied torque.

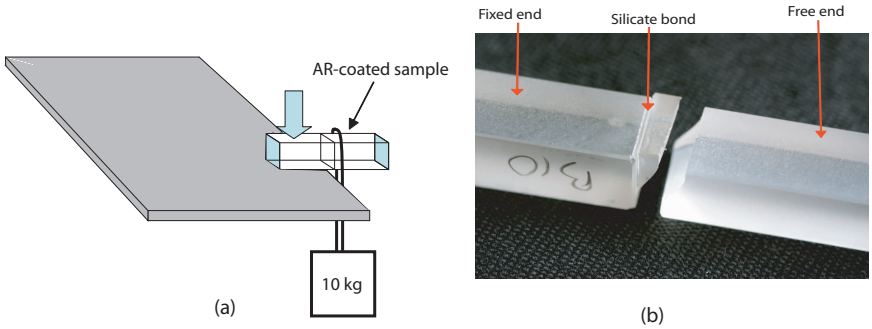

Fig. 13. (a) Setup for measuring shear strength of silicate bonded samples. Weights from 5 kg to 25 kg were used to apply stress in our setup. (b) Photograph showing one of the silicate-bonded samples that fractured.

The three random samples fractured when loaded with weights of 40 pounds, 41 pounds and 43 pounds. With a bonded area of 30 mm^2, this corresponds to an average shear strength of 0.63 kg/mm^2, which compares very favorably to silicate-bond strengths reported by other research groups [9]. Although this measured shear strength of the bond is almost an order of magnitude below the reported shear strength value of fused silica, the fractures from all three samples propagated to the bulk of the samples. Furthermore, one of the samples fractured in two different places in the bulk with no observable damage along the bond. One possible explanation for this behavior is that, despite our efforts, we were applying far more torque to the samples than we had intended. In this case, the 0.63 kg/mm^2 measured shear strength value should be treated as a lower bound. A photograph of one of the fractured samples is shown in Fig. 13(b). The fracture began in the bulk of the free end of the sample. The fracture then propagated towards the bond. The break crossed the bond into the fixed end of the sample at the end of the break. Silicate bonds have been shown to be at least as strong in tension as in shear [20].

As shown in Fig. 1, we propose to place the gain fiber into a capillary which is then polished and bonded to the flat. The surface area of the thick-walled capillary is approximately 36 mm^2. Thus, given our shear strength of 0.63 kg/mm^2, our fiber-bonded structures should be able to handle a shear stress corresponding to masses of 22.7 kg, which is sufficient for most industrial environments.

#86286 - $15.00 USD Received 10 Aug 2007; revised 14 Sep 2007; accepted 24 Sep 2007; published 25 Sep 2007

8. Summary

In this paper, we demonstrated how silicate bonding optical flats to fiber facets can increase the reliability of high-power fiber systems by decreasing the optical fluence at the silica-air interface. Damage thresholds at the silicate bond in excess of 70 J/cm^2 with 25 ns pulses at a wavelength 1064 nm were measured for samples that were bonded with optimal bonding parameters. We also illustrated how silicate bonding can be used to dramatically reduce the effective feedback at the output of double-clad fibers. We verified experimentally that the Fresnel reflection from the silicate bond can be below -63 dB. Furthermore, we discussed how the feedback reduction allowed by silicate bonding does not depend on the fiber outer diameter. This allows the use of large cores with small claddings for efficient pump absorption while maintaining extremely low feedback levels. In addition, silicate bonding allows low feedback without the need for angled end-facets. In circular fibers, this minimizes the ellipticity of the output beam and therefore it reduces the cost and complexity of the optical imaging system needed to efficiently mode match the output beam from the fiber to resonant cavities with circular eigenmodes (such as the LIGO pre-mode cleaners locked on the TEM_{00} mode) [21].

By exploring a large operating space, we determined that the optimum silicate bonding conditions to simultaneously maximize the damage threshold and minimize the Fresnel reflection involved using a sodium trisilicate solution that is diluted to 16.7% by volume with a total applied solution volume of 0.10 μL/mm^2. The bonded samples should be cured at a temperature between 90°C and 120°C for 8 hours. We also demonstrated that the shear strength of the silicate bond (0.63 kg/mm^2) should be sufficient for most operating environments.

Appendix A: Procedure for silicate bonding fused silica samples

The cross-sectional area of most gain fibers is too small to provide the necessary mechanical support to enable polishing and bonding of the fiber end to a thick optical flat. Thus, to increase the surface area of the bonding surface on the fiber end, we bond the last few centimeters of the fiber length into a fused silica capillary with UV-curable epoxy. The fiber end and the capillary face is polished flat to allow bonding to the optical flat. A photograph of such a bonded sample is shown in Fig. 1(b).

Cleanliness of the surfaces to be bonded, purity of the sodium silicate solution, and quality of the polish (especially flatness) are key for successful silicate bonding. We used the following procedure to silicate bond optical samples:

1. The surfaces to be bonded (i.e., the optical flat and the optical fiber in the capillary) should be polished as flat as possible (preferably to better than 100 nm peak-to-valley flatness). We typically use a pitch polish for the final step (once the lap polish achieves a flatness of better than a wavelength).
2. Bring samples to an area that meets or exceeds class-100 cleanroom specifications.
3. Dilute 10 mL of reagant-grade sodium trisilicate solution (27% as SiO_2) to the desired concentration with de-ionized (DI) water in a clean vial.
4. Manually shake the vial rigorously for 30 seconds and then pour the well-mixed solution into a syringeless filter (with 0.2 μm-nylon membrane filter).
5. Plunge particulate-filtered solution into a small clean resealable vial.
6. Saturate a low particulate generating cleanroom wipe with a zirconium oxide water-based paste and scrub the surfaces to be bonded for 30 seconds.
7. Rinse the surfaces thoroughly with DI water and wipe with a clean cleanroom wipe.
8. Saturate a low particulate generating cleanroom wipe with a sodium bi-carbonate water-based paste and scrub the surfaces to be bonded for 30 seconds.

#86286 - $15.00 USD Received 10 Aug 2007; revised 14 Sep 2007; accepted 24 Sep 2007; published 25 Sep 2007

9. Rinse the surfaces thoroughly with DI water and wipe with a clean cleanroom wipe.
10. Wipe the surfaces to be bonded with a low particulate generating cleanroom wipe wetted with methanol.
11. Inspect surfaces with high brightness white light source.
12. Using a calibrated pipette with a clean, disposable tip, draw out the desired amount of solution from the resealable vial and place on one of the surfaces to be bonded.
13. Bring the two surfaces in contact and ensure no air bubbles are formed.
14. After two days, place the samples in a soft vacuum with a dessicant for one day to accelerate the dehydration process.
15. The samples can begin their temperature curing cycle in an ambient air furnace after two days. The duration of the curing cycle and the slope of the temperature ramp depends on the size of the samples that are being bonded. For the samples that we characterize in detail in this paper, the temperature was increased at a rate of 100°C/hour until the desired curing temperature was reached. The furnace held this temperature for 4 hours, after which the temperature was ramped down at a rate of 100°C/hour.

We use a silicate bonding solution instead of a hydroxide bonding solution because the silicate solution has been experimentally found to have a greater tolerance to flatness errors during the bonding process [9].

Acknowledgments

We would like to thank Romain Gaume, Sheila Rowan, Caroline Cantley, and Helena Armandula for several helpful discussions. This research is based upon work supported by the U.S. Army Research Office under ARO contract DAAD19-01-1-0184.

#86286 - $15.00 USD Received 10 Aug 2007; revised 14 Sep 2007; accepted 24 Sep 2007; published 25 Sep 2007